AAPM REPORT NO. 28

QUALITY ASSURANCE METHODS AND PHANTOMS FOR MAGNETIC RESONANCE IMAGING

Published for the
American Association of Physicists in Medicine
by the American Institute of Physics

AAPM REPORT NO. 28

QUALITY ASSURANCE METHODS AND PHANTOMS FOR MAGNETIC RESONANCE IMAGING[†]

REPORT OF
TASK GROUP NO. 1
NUCLEAR MAGNETIC RESONANCE COMMITTEE*

AAPM

Members

Ronald R. Price (Task Group Chairman)
Leon Axel
Tommie Morgan
Robert Newman
William Perman
Nicholas Schneiders
Mark Selikson
Michael L. Wood[‡]
Stephen R. Thomas

[†] Reprinted from MEDICAL PHYSICS, Volume 17, Issue 2, 1990

*Ronald R. Price, Nuclear Magnetic Resonance Committee Chairman
Stephen R. Thomas, Past Committee Chairman

[‡] Michael L. Wood, Current Task Group Chairman

May 1990

Published for the
American Association of Physicists in Medicine
by the American Institute of Physics

Further copies of this report may be obtained from:

American Institute of Physics
c/o AIDC
64 Depot Road
Colchester, Vermont 05446

(1-800-445-6638)

International Standard Book Number: O-8831 8-800-7
International Standard Serial Number: 0271-7344

Published by the American Institute of Physics, Inc.
335 East 45 Street, New York, NY 10017

Printed in the United States of America

Quality assurance methods and phantoms for magnetic resonance imaging: Report of AAPM nuclear magnetic resonance Task Group No. 1[a]

Ronald R. Price, Leon Axel, Tommie Morgan, Robert Newman, William Perman, Nicholas Schneiders, Mark Selikson, Michael Wood, and Stephen R. Thomas
AAPM Task Group No. I

(Received 6 September 1989; accepted for publication 30 October 1989)

I. INTRODUCTION

The purpose of this document is to describe a standard set of test procedures which can be used to evaluate the performance of clinical magnetic resonance imaging systems. These procedures and tests are not intended to establish absolute performance standards but are rather intended to provide methods which can be used as part of a routine quality assurance program. It is the position of this document that the purpose of a quality assurance program is to detect changes in system performance relative to an established baseline.

This document also includes recommendations for acceptable magnetic resonance imaging (MRI) phantom materials, phantom designs, and analysis procedures. Specific image parameters described in ths document are: resonance frequency, signal-to-noise, image uniformity, spatial linearity, spatial resolution, slice thickness, slice position/separation, and phase related image artifacts. It is recognized that this set is not exhaustive and does not include procedures for assessing all possible image parameters, and similarly it is also recognized that there are acceptable methods other than those presented for measuring many of these parameters. The proposed set, however, is considered to be adequate for monitoring the sensitivity and geometric characteristics of clinical nuclear magnetic resonance (NMR) imaging systems.

The proposed set does not include specific procedures for monitoring the accuracy or precision of T1, T2 or proton density. Since at the present time, there are no commonly accepted standard methods for determining T1, T2 and proton density from image data and the assessment of these parameters is not currently a part of clinical practice, we have chosen not to include these test procedures until more knowledge on their utility and measurement is available.

The National Electrical Manufacturers Association (NEMA) is acknowledged for their assistance in the development of the sections on field uniformity and signal-to-noise. The specifications for these two parameters are consistent with the NEMA specifications wherever possible under the requirement that the procedures are applicable for use in a practical quality assurance program. The American College of Radiology (ACR) Subcommittee on Magnetic Resonance (MR) Nomenclature and Phantom Development under the MR Committee on Imaging Technology and Equipment is acknowledged for its persistent and careful review over the several years that this document has been under development.

II. PHANTOM MATERIALS

The primary considerations which dictate the choice of phantom materials for use in quality assurance phantoms are: chemical and thermal stability, the absence of significant chemical shifts, appropriate T1, T2 and proton density values which are within the biological range. As will be noted later, coil loading is an important consideration when assessing signal-to-noise. Other considerations generally relate to convenience and practicality: convenience by matching the T1 of the material to an acceptable TR which does not require an exceedingly long scan time and practicality by not choosing a T2 value shorter that some instruments can accommodate. Care should be taken to avoid the use of colored plastics or other container materials which possess significantly different magnetic susceptibility from the filler material.

At each operating field strength, it is recommended that the chosen NMR material should exhibit the following characteristics:

$$100\text{ms} < T1 < 1200\text{ms}$$
$$50\text{ms} < T2 < 400\text{ms}$$
$$\text{proton density} \approx H_2O \text{ density}$$

Numerous materials have been used successfully as NMR phantom agents. These have primarily consisted of oils and water solutions of various paramagnetic ions. For reference, listed in Table I are approximate relaxation times for mixtures of 1,2 propanediol in distilled water (Ref. 1) and three paramagnetic agents [$CuSO_4$(Ref. 2)) $NiCl_2$(Ref. 2) and $MnCl_2$(Ref. 3)] at 20 MHz (0.5 T). It should be noted that relaxation times are temperature and field-strength dependent.

The relaxation rates (inverse of relaxation times) are approximately linear with ion concentration.

For all measurements, scan conditions should be carefully recorded. Scan conditions should include: pulse sequence and scan timing parameters (TE, TI, TR), flip angle, field-of-view and matrix size, coil, phantom and phantom material, slice number and thickness, center-to-center spacing, number of acquisitions, rf power settings and any image processing which may have been used. All phantoms should be centered at the magnet isocenter unless otherwide specified.

Action criteria listed in this document are for reference only. Absolute values of quality control parameters are ma-

 0094-2405/90/020287-09S01.20

TABLE I. Approximate relaxation times of NMR phantom materials.

Agent	Concentration	T1	T2
$CuSO_4$	1-25 mM	860-40 ms	625-38 ms
$NiCl_2$	1-25 mM	806-59 ms	763-66 ms
Propanediol	0-100%	2134-217 ms	485-72 ms
$MnCl_2$	0.1-1 nM	982-132 ms	...

chine dependent and as a result, make it impossible to specify action criteria which can be applied universally to all systems. Specific action criteria must be arrived at individually for each system installation in cooperation with the user and instrument manufacturer.

III. RESONANCE FREQUENCY

A. Definition

The resonance frequency is defined as that rf frequency f which matches the static B-field (B_0) according to the Larmor equation:

$$f = \frac{\gamma}{2\pi} B_0,$$

g is the gyromagnetic ratio for the nuclei under study. For protons, the Larmor frequency is 42.58 MHz/T, e.g., for a 1.5-T system, the resonance frequency should be 63.87 MHz.

B. Factors affecting resonance frequency

Prior to the performance of any imaging protocol, it is essential that the operator verify that the system is on resonance. Most vendors insist upon a resonance frequency check each time the imaging system is turned on. Resonance frequency checks are most important for mobile units and some resistive magnet systems which undergo frequent ramping of the magnetic field. Changes in the resonance frequency reflect changes in the static B-field. Changes in the static B-field may be due to superconductor "run down" (typically on the order of 1 ppm/day, e.g., ~60 Hz/day at 1.5 T), changes in current density due to thermal or mechanical effects, shim-coil changes or effects due to external ferromagnetic materials.

The effects of off-resonance operation relate primarily to system sensitivity and are manifest as a reduction in image signal-to-noise. Secondary effects are reflected in image linearity due to the summation of the image gradients with the inconsistent static B-field value.

It is recommended that a resonance frequency check be performed prior to quality assurance measurement and each time a different phantom is used.

C. Methods of Measurement

1. Phantom

The phantom which is used most often for resonance frequency checks in a uniform signal producing cylinder and is the same phantom that is used for the signal-to-noise measurements. The phantom is positioned in the center of the magnet (with all gradient fields turned off) and the rf frequency is adjusted by controlling the rf synthesizer center frequency to achieve maximum signal. Some resistive systems may also allow adjustment of the magnet current to alter the magnetic field strength to achieve resonance. Most vendors will provide a specific user protocol for resonance frequency adjustment and some may be completely automated. Resonance frequency should be recorded daily for trend analysis.

2. Scan conditions

No scan is required for this measurement.

3. Analysis

Resonance frequency value is recorded for comparison to previous determinations.

D. Action criterion

Values of resonance frequency should generally not deviate by more than 50 ppm between successive daily measurements. Action should also be taken any time there is a significant change in trend.

IV. SIGNAL-TO-NOISE RATIO

A. Definition

The signal is defined as the mean pixel value within the region-of-interest minus any pixel offset. Noise is defined as the random variations in pixel intensity. Images with obvious artifacts are not suitable for signal-to-noise determinations.

B. Factors affecting signal-to-noise ratio

Factors contributing to variations in signal-to-noise ratio include: (i) general system calibration (resonance frequency, flip angles, etc.) (ii) gain, (iii) coil tuning, (iv) rf shielding, (v) coil loading, (vi) image processing, and (vii) scan parameters.

C. Methods of measurement

1. Phantom

The phantom should consist of a uniform signal producing material which has a minimum dimension in the image plane of at least 10 cm or 80% of the field-of-view, whichever is larger (Fig. 1). For single slice measurements, the phantom should have a dimension in the direction of the slice selection which is at least twice the maximum slice thickness being used. For multislice acquisitions, the phantom length should be at least as long as the volume being imaged, plus two maximum slice thicknesses. The phantom may be either circular or rectangular in cross section. When using large volume fluid-filled phantoms, it should be recognized that thermal and mechanically induced motions can introduce artifacts.

The standard phantom specified here is to be filled with nonconducting material, and thus is not intended to simulate the clinical situation. The unloaded coil allows the evaluation of system noise which is the parameter of interest. In a

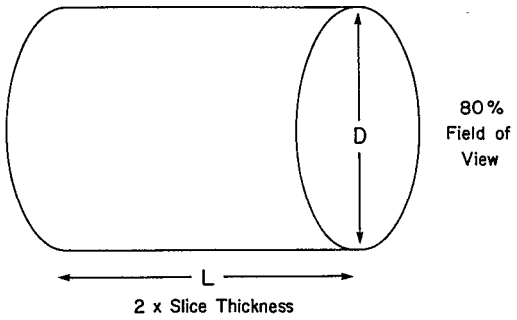

FIG. 1. The phantom used for resonance frequency, signal-to-noise ratio and image uniformity is typically composed of a uniform signal producing material. The minimum dimension *(D)* in the image plane should be at least 10 cm or 80% of the image field-of-view, whichever is larger. The length *(L)* in the slice selection direction should be at least twice the maximum slice thickness for single-slice measurements. For multislice measurements, *L* should be at least as long as the volume being imaged (slice separation- x number of slices), plus a thickness equal to twice the maximum slice thickness.

clinical scan, it is recognized that the patient is the dominant source of noise. In order to approximate the clinical situation, the coil must be electrically loaded by using an appropriate filler material or by some other means, whereby the electrical properties of the body are simulated.

Worthy of note is that the NEMA standard for signal-to-noise does specify loading for the measurement and thus differs from the signal-to-noise measurement specified in this document. It should also be noted that systems with certain high-Q coils may not be tunable under unloaded conditions.

2. Scan conditions

Any typical (usually multislice) acquisition may be used.

3. Analysis

The signal is measured using a region of interest (ROI) which contains at least 100 pixels or 10% of the area of the signal producing material, whichever is greater. The ROI should be positioned in the center of the image and should not include any obvious artifacts. The signal is the mean value of the pixel intensity in the ROI minus any offset. (An indication of the existence of an image intensity offset may be gained from an examination of intensity values from ROI's taken over nonsignal producing portions of a phantom. Specific offset values should be obtained from the system manufacturer). The noise is the standard deviation derived from the same ROI. The signal-to-noise ratio (SNR) is then calculated.

An alternative method of SNR measurement is to acquire two consecutive scans with identical scan parameters which are subsequently subtracted. This method specifically excludes the effects of low-frequency image variations. A third pixel-by-pixel difference image (image 3) is then created. The signal is defined as above using either of the original unsubtracted images. The noise is defined as the standard deviation (SD) derived from using the same ROI on the subtracted image (image 3).

The calculated signal-to-noise is as follows:

$$\mathrm{SNR} = \frac{S\sqrt{2}}{\mathrm{SD}}$$

The factor of $\sqrt{2}$ is required because the SD is derived from the subtraction image rather than from one of the original images.[4]

D. Action criterion

An action criterion can not be given since SNR results are only applicable to the specific system, phantom and scan conditions being used. It is important to re-emphasize that the signal and noise measurements are dependent on essentially all scan parameters and test conditions. SNR should be normalized to voxel size for comparison.

V. IMAGE UNIFORMITY

A. Definition

Image uniformity refers to the ability of the MR imaging system to produce a constant signal response throughout the scanned volume when the object being imaged has homogeneous MR characteristics.

B. Factors affecting image uniformity

Parameters contributing to the image nonuniformity include: (i) static-field inhomogeneities, (ii) rf field non-uniformity, (iii) eddy currents, (iv) gradient pulse calibration, and (v) image processing.

C. Methods of measurement

1. Phantom

The characteristics of the phantom used for image uniformity evaluation are identical to the characteristics of the phantom used for signal-to-noise determination (Sec. IV). To prevent rf penetration effects, the filler material should be non-conducting.

Nonuniformities resulting from rf penetration effects may be evaluated by scanning a phantom which has been filled with a conductive solution such as normal saline. Due to partitioning in the body, penetration effects observed in a scan of a saline-filled phantom will not necessarily predict penetration effects which would be found in human scans.

2. Scan conditions

Any typical multislice acquisition may be used provided the signal-to-noise ratio is sufficiently large so that it does not affect the uniformity measurement. Adequate signal-to-noise ratio may be insured by either increasing the number of acquisitions or by applying a low-pass smoothing filter. In practice, it has been found that a signal-to-noise ratio of 80:1 or greater will yield good results.

3. Analysis

For pixels within a centered geometric area which encloses approximately 75% of the phantom area, the maxi-

mum (S_{max}) and minimum (S_{max}) values are determined. Care should be taken to not include edge artifacts in the ROI. A span A and midrange value $\overline{S}$ are calculated as follows:

$$\Delta = \frac{S_{\max} - S_{\min}}{2}$$

$$\overline{S} = \frac{S_{\max} + S_{\min}}{2}.$$

The relationship for calculating integral uniformity (U_s) is

$$U_\Sigma = \left[1 - \frac{\Delta}{\overline{S}}\right] \times 100\% = \left[1 - \frac{(S_{\max} - S_{\min})}{(S_{\max} + S_{\min})}\right] \times 100\%.$$

Perfect integral uniformity using this relationship is when $U_s = 100\%$.

In some cases (e.g.. low-field imaging) signal-to-noise may be a limiting factor in the measurement of image uniformity. To help minimize the effect of noise on the measurement the image may be convolved with a nine-point low-pass filter $h(m_1,m_2)$. The filtered image is given by

$$s(n_1,n_2) = \frac{1}{W} \sum_{m_1=-1}^{1} \sum_{m_2=-1}^{1} h(m_1,m_2) s(n_1 - m_1, n_2 - m_2),$$

where *n1, n2* cover the range of the image.

The filter kernel is

$$\frac{1}{W}\begin{bmatrix} 1 & 2 & 1 \\ 2 & 4 & 2 \\ 1 & 2 & 1 \end{bmatrix} = \begin{bmatrix} h(-1,-1) & h(-1,0) & h(-1,1) \\ h(0,-1) & h(0,0) & h(0,1) \\ h(1,-1) & h(1,0) & h(1,1) \end{bmatrix},$$

and represents the product of two raised cosines in the frequency domain. The weighting factor W is given by

$$W = \sum_{m_1=-1}^{1} \sum_{m_2=-1}^{1} h(m_1,m_2) = 16,$$

and is used to normalize the dc response of the filter in the frequency domain to unity. This filter has a 3-dB cutoff spatial frequency contour which very closely approximates a circle of radius 0.364 π in normalized coordinates. It is the two-dimensional equivalent of the Hanning filter. The above filter gives a gain in the signal-to-noise ratio of 2.4.

D. Action criterion

For a 20-cm field-of-view or less, the integral uniformity should be typically 80% or better. It should be realized that for larger fields-of-view, the uniformity may deteriorate. Image uniformity in the above context is not defined for surface coils.

VI. SPATIAL LINEARITY

A. Definition

Spatial linearity is a term used to describe the degree of geometrical distortion present in images produced by any imaging system. Geometrical distortion can refer to either displacement of displayed points within an image relative to their known location, or improper scaling of the distance between points anywhere within the image.

B. Factors affecting spatial linearity

The primary factors which introduce geometrical distortion in NMR imaging are: (i) inhomogeneity of the main magnetic field and; (ii) nonlinear magnetic field gradients.

C. Methods of measurement

1. Phantom

Variability is best observed over the largest field-of-view. The phantom to be used to measure spatial linearity should occupy at least 60% of the largest field-of-view and consist of a regular array of objects (holes, grooves, rods, or tubes) of known dimensions and spacing, and the phantom filled with signal producing material. The objects within the array should be of a size in which the location can be measured and spaced in a regular pattern (typically every 1-2 cm). The dimensional positioning error of the objects within the array, due to finite pixel size, should be < 10% of the linearity specification. Figure 2 provides an illustration of two possible patterns which could be used to evaluate spatial linearity.

2. Scan conditions

Consideration should be given to determining the spatial linearity for a typical multislice acquisition with the largest available image matrix to maximize spatial resolution.

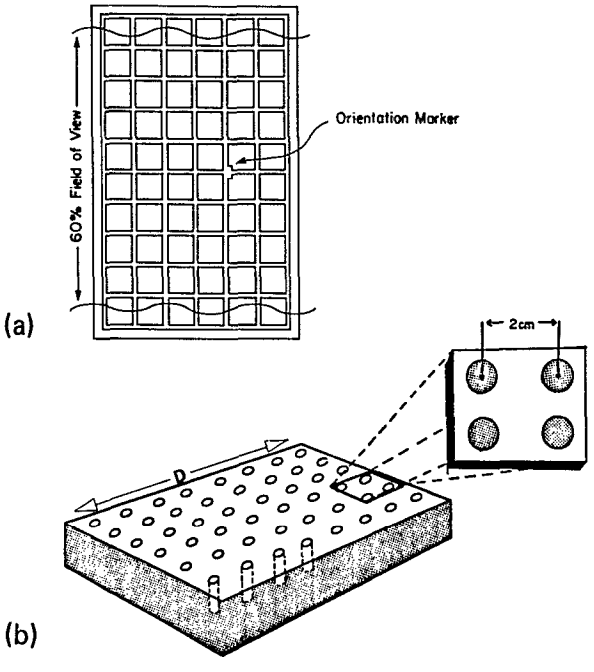

FIG. 2. The phantom used for spatial linearity should have a minimum dimension *(D)* in the image plane of at least 60% of the largest possible image field-of-view. The thickness of the phantom should be at least twice the maximum slice thickness for single-slice measurements and two slice thicknesses, plus the image volume length for multislice measurements. Two possible phantom designs are (a) orthogonal grooves in an acrylic plate of (b) an orthogonal array of holes drilled in an acrylic plate. Orientation markers are recommended.

Since NMR imaging is inherently a volumetric imaging technique, the evaluation should be performed for each orthogonal plane to define the useful imaging volume. This can be done either by using a specially designed phantom for multislice image acquisition or by using a single-slice phantom placed at different locations and in the three orthogonal orientations. Spatial linearity is not expected to depend significantly on image timing parameters such as TE, TR and the number of signal acquisitions.

If oblique planes are frequently used, consideration should be given to the inclusion of linearity measurements for oblique planes, as well as the orthogonal planes.

3. *Analysis*

Percent distortion is defined as

$$\frac{\text{true dimension} - \text{observed dimension}}{\text{true dimension}} \times 100\%.$$

Distortion measurement may be performed between any two points within the field-of-view, provided that pixel-resolution is not a significant source of error. It is recommended that the true dimension be greater than 10 pixels. Preliminary considerations by the NEMA task group to specify image distortion have centered on the use of a cylindrical phantom in which several measured diameters are compared to the known diameter. Specification in terms of the maximum deviation (maximum-minimum) expressed as a percent of the known diameter is also under consideration.

Spatial linearity measurements performed directly on the image processing unit will provide information about the MR imaging system alone. Measurements can also be performed upon filmed images and will provide combined performance information about the MR imager, as well as the video and filming systems.

D. Action criterion

Percent distortions in the spatial linearity (when measured over a 25 cm or greater field-of-view) are generally considered acceptable if they are < 5%.

VII. HIGH-CONTRAST SPATIAL RESOLUTION

A. Definition

High-contrast spatial resolution is a measure of the capacity of an imaging system to show separation of objects when there is no significant noise contribution. High-contrast spatial resolution for MRI systems is typically limited by acquisition matrix pixel size (field-of-view divided by the sampling in *x* or *y).* The acquisition matrix pixel size should not be confused with the display matrix pixel size in which pixel interpolation or replication may have occurred.

Traditionally, resoltuion has been quantified by the point spread function (PSF), line spread function (LSF), or modulation transfer function (MTF); however, these methods are not practical for routine quality assurance measurements on MRI systems. Therefore, a visual evaluation of test objects will be used.

B. Factors affecting resolution

Factors contributing to high-contrast resolution include: field-of-view (determined by gradient strength and sampling period), acquisition matrix and reconstruction filters.

C. Methods of measurement

1. *Phantom*

Useful spatial resolution phantoms for visual evaluation may be composed of either bar patterns or hole (or rod) arrays. Array signal-producing elements may be either round or rectangular in cross section. The patterns consist of alternating signal producing and nonsignal producing areas set apart from each other by a width equal to the bar's or hole's width, i.e., center-to-center spacing is twice the diameter. Square bar patterns offer an advantage over round cross-section (hole) patterns in that the smallest resolvable array element can be related to resolution in terms of line-pairs per millimeter.

A typical phantom (Fig. 3) may consist of five signal producing elements and four spaces with element sizes of 5, 3, 2, 1.5, 1.25, 1.00, 0.75, and 0.50 mm, although additional increments may be used. The dimension in the slice selection direction (length) should be at least twice the slice thickness, i.e., 20 mm length for 10 mm slice thickness.

2. *Scan conditions*

Any typical multislice acquisition may be used provided it incorporates an appropriate slice thickness (nominal 5-10 mm) to insure an adequate signal-to-noise. The phantom should be aligned perpendicular to the scan plane and locat-

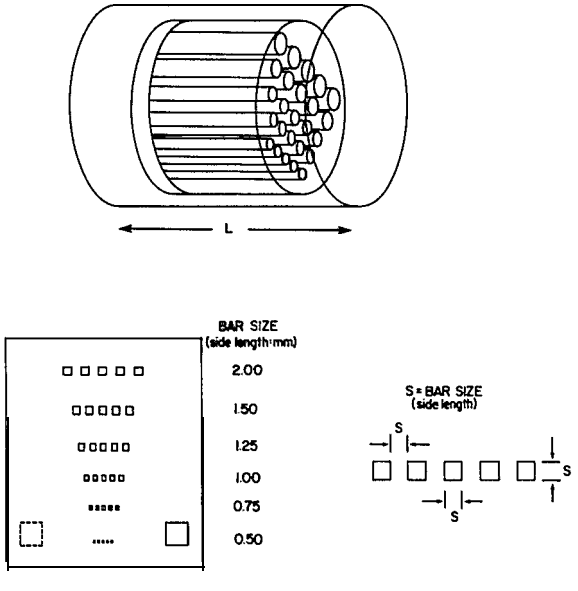

FIG. 3. High-contrast resolution phantoms may be composed of either bar patterns or hole arrays. Bars or holes should have center-to-center spacings *(S)* equal to twice the hole diameter or bar dimension. Thelength *(L)* of the phantom should be at least twice the maximum slice thickness. Bars derived from grooves in an acrylic sheet may be preferred due to construction difficulties.

ed at the isocenter and should be rotated at 45° within the image plane to combine the resolution from both the phase and frequency encoding directions. In order to determine the resolution in the phase and frequency encoding directions independently, two scans will be required in which the phantom resolution elements are aligned along each axis separately and then scanned.

3. Analysis

The image will be evaluated visually. Image analysis consists of viewing the image to determine the smallest resolvable array element (magnification may be used if desired). For an array to be resolved, all five elements and four spaces must be displayed as separate and distinct when viewed with the narrowest window width. The window level should be adjusted for optimum visualization. Resolution is expressed as the size of the smallest resolvable array element or its equivalent in lp/mm when square bar patterns are used.

D. Action criterion

The high-constrast resolution should remain constant for repeated measurements under the same scan conditions and should be equal to the pixel size. For example for a 25.6 cm field-of-view with a 256x256 acquisitions matrix, the resolution should be 1 mm.

VIII. SLICE THICKNESS

A. Definition

Slice thickness is defined as the full width at half-maximum (FWHM) of a slice profile. The full width at tenth-maximum (FWTM) is an additional descriptor of the slice profile. The slice profile is defined as the response of the magnetic resonance imaging system to a point source as it moves through the plane of the reconstruction at that point.

B. Factors affecting slice thickness

(i) Gradient field nonuniformity, (ii) rf field nonuniformity, (iii) nonuniform static magnetic field, (iv) noncoplanar slice selection pulses between excitation and readout, (v) TR/T1 ratio, and (vi) rf pulse shape and stimulated echoes.

C. Methods of measurement

1. Phantoms

Several phantoms can be used to evaluate slice thickness, most of which utilize some variant of an inclined surface (plane, cone or spiral). A typical phantom is the crossed high signal ramps.

High signal ramp (HSR) phantoms generally consist of opposing ramp pairs oriented at a fixed angle (Θ) [Fig. 4(a)] with respect to one another. The HSR's should be thin (ideally infinitesimally thin) in order to quantify the slice profile accurately. Because of the low signal in the image imposed by the small volume of signal-producing material in a thin ramp, averages of pixel values across the width of the ramp may be needed to generate a slice profile with an acceptable SNR. As thinner (< 3 mm) slice thicknesses are evaluated, it is necessary to increase ramp angle and to decrease ramp thickness. In general, the thickness of a (90°) HSR oriented at 45° respect to the image plane should be < 20% of the slice profile FWHM (i.e., 5-mm slice needs a l-mm ramp) to get a measurement with < 20% error.

An alternative method which is particularly useful for evaluating thin slices is the use of the slice selection echo method.[5] A standard selective 90° and 180° pulse sequence may be used together with a readout gradient oriented along the slice selection direction. The Fourier transform of the resulting echo gives a picture of the slice profile. The strength of the readout gradient is needed to translate the frequency axis to actual spatial dimensions.

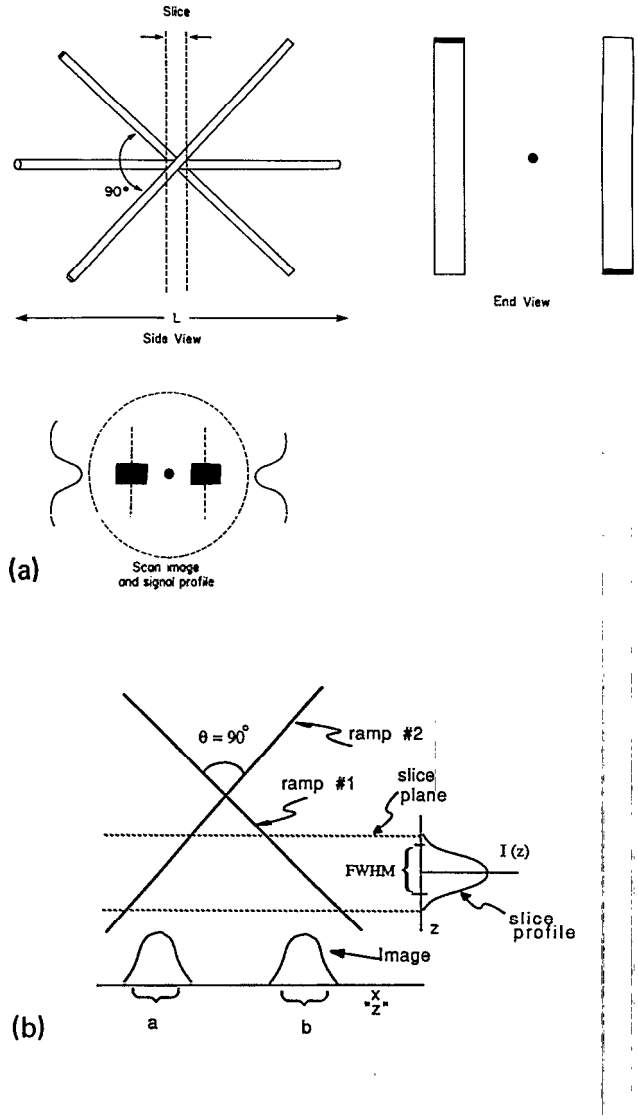

FIG. 4. (a) A typical slice-thickness phantom consists of two crossed thin ramps. A ramp crossing angle of 90° yields an angle of 45° between the ramp and the image plane. Ramp thickness should typically be < 20% of the slice thickness being evaluated. Phantom length *(L)* should be greater than twice the maximum slice thickness. An alignment rod passing between the two ramps defines the point where the two ramps cross. When the slice is properly aligned through the intersection of the ramps the images of the ramps and rod image will all be aligned. (b) The slice sensitivity profile will be directly proportional to the image intensity profiles if the image plane is perpendicular to the alignment rod. By using the geometric mean of the two profiles ($\sqrt{ab}$) correct FWHM values are obtained even with image plane misalignment.

2. Scan conditions

Any typical multislice acquisition may be used provided TR is greater than 3T1 of the filler material and the highest pixel resolution is used. Slice thickness should be measured both centrally and peripherally within an image and at both central (magnet isocenter) and offset slice locations.

3. Analysis

Slice thickness (FWHM, FWTM) : In the resultant image, the signal level is read out across the ramp on a pixel-by-pixel basis along a line-of-interest oriented orthogonally to the ramp width dimension. As noted previously, to assure adequate S/N, it may be necessary to either use multiple excitations or several line profiles. The FWHM or FWTM parameters should be determined for each of the dual ramps.

The general equation for the FWHM from imaging opposed high signal ramps (relative angle Θ) oriented at any angle with respect to the image plane is

$$\mathrm{FWHM} = \frac{(a+b)\cos\Theta + \sqrt{(a+b)^2\cos^2\Theta + 4ab\sin^2\Theta}}{2\sin\Theta}$$

where a and b refer to the measured FWHM (FWTM) of the intensity profiles for ramp 1 and ramp 2, respectively [Fig. 4(b)].[6]

For the case of $\Theta = 90°$, the equation simplifies to:

$$\mathrm{FWHM} = \sqrt{ab}$$

D. Action criterion

Assuring adequate measurement accuracy, the measured value of slice thickness should generally agree with the indicated slice thickness within ± 1 mm for slice thicknesses > 5 mm.

IX. SLICE POSITION/SEPARATION

A. Definition

Slice position (offset) is the absolute location of the midpoint of the FWHM of the slice profile. Slice separation is the distance between any two slice positions. Slice locations are indicated by external positioning devices or by the selected interslice spacing.

B. Factors affecting slice position/separation

(i) Misalignment of positioning devices, (ii) gradient field nonuniformity, (iii) B1 nonuniformity, (iv) noncoplanar slice selection pulses, and (v) static magnetic field.

C. Methods of measurement

1. Phantoms

In general, the same phantom used for slice thickness measurements [Fig. 4(a)] may also be used for slice position/separation determinations, with the provision that the phantom contains reference pins and external scribed marks for orientation, centering, and reference to the external positioning devices. An inclined surface, with a known pitch, when imaged at different locations will produce images which will be displaced relative to a reference in direct proportion to the slice location and the pitch of the surface.

2. Scan conditions

Any typical acquisition is suitable for slice position/separation determinations.

3. Analysis

The midpoint of the FWHM of the slice profile in the image of interest is determined. (Fig. 5). The distance *(D)* from the profile midpoint to a landmark (alignment rod) which remains stationary from slice-to-slice (parallel to the slice selection direction) is measured and related to the slice position *(O)*. For a 45° ramp, the distance from a centered reference pin to the slice profile midpoint will be equal to the slice distance from the magnet isocenter if the phantom is accurately positioned with the crossover point of the ramps located at the isocenter. For any relative ramp angle (Θ) the slice offset position *(O)* will be given by

$$O = D / \tan(\Theta / 2).$$

All measurements should be made along the line defined by the magnet isocenter and the centers of the imaging planes.

D. Action criterion

Comparison of external position marker should generally agree with the actual slice position within ± 2 mm. Slice separation disagreement should typically be < 20% of the total slice separation or ± 1 mm, whichever is greater.

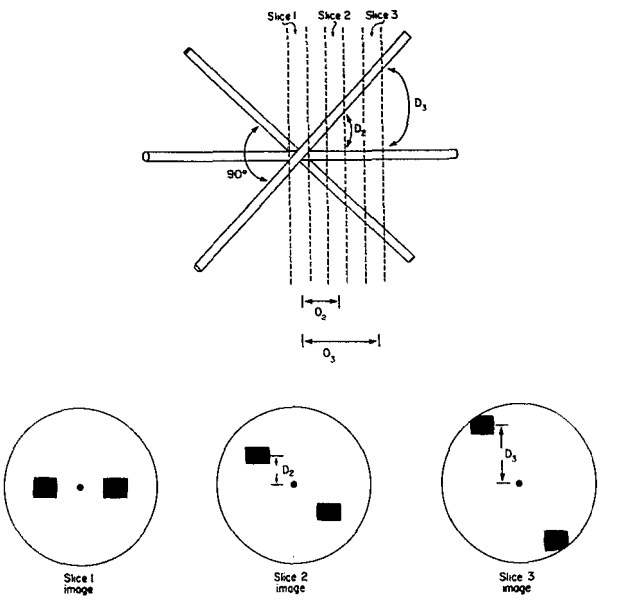

FIG. 5. Slice position (offset) and separation may be determined using a phantom similar to the slice-thickness phantom (Fig. 4). Slices taken at different locations (0,) (slices l-3) in a multislice sequence will produce images of the ramps which are progressively further from the alignment rod *(D)*. The distance D is measured in the image and then related to the true slice location *(O)* from the isocenter.

X. IMAGE ARTIFACTS

A. Definition

Phase related errors are defined in terms of inappropriate (either increased or decreased) image signal at specified spatial locations. Generally, these artifacts are characterized by increased signal intensity in areas which are known to contain no signal producing material. Commonly called "ghosts", errors in the application of phase-encoding gradients for imaging and errors in both rf transmit and receive quadrature phase, result in unique ghost artifacts. A "dc-offset" error is defined here as high-intensity or low-intensity pixels at the center of the image matrix due to improper scaling of low-frequency components (typically dc) in the Fourier transformation of the NMR time-domain signal.

B. Factors affecting phase related artifacts

(i) Phase encoding gradient instability, (ii) quadrature phase maladjustment in the synthesis of slice selective rf pulses (transmit error), and (iii) improper quadrature phase decoding on receive.

C. Methods of measurement

1. Phantom

A typical phantom design is illustrated in Fig. 6. It consists of a single signal producing cylinder (2-5 cm) located at an asymmetric location, typically on the periphery of the field-of-view at a 45° orientation. The phantom thickness should be approximately twice the slice thickness being used. Orientation markers are particularly beneficial for this phantom.

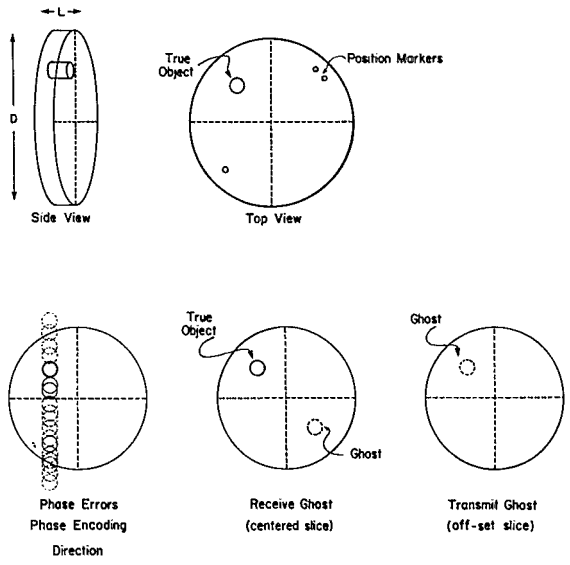

FIG. 6. A typical phantom for quadrature error detection consists of a single signal producing cylinder (labeled "true-object") located at an asymmetric location, e.g., at the periphery of the field-of-view at a 45° orientation. The size of the cylinder is not critical and may be as large as 2-5 cm in diameter. Marker sources are important for orientation information. Phantom diameter *(D)* should be at least 10 cm. Phantom thickness *(L)* should be at least two times the maximum slice thickness.

2. Scan conditions

Any typical multislice sequence may be used. Separate scans must be made to assess both transmit and receive errors if a phantom similar to the phantom in Fig. 5 is used. More complex volume phantoms may be designed in which both transmit and receive errors may be assessed with a single-scan sequence. The scan for assessing receive quadrature errors is made with the phantom placed at the magnet isocenter with the central slice of the multislice sequence passing through the phantom. The same scan may be used to assess both dc-offset and phase encoding errors. The scan for assessing transmit quadrature errors is made with the phantom placed at a convenient offset slice position (typically ± 5 cm from the isocenter slice) with the center slice passing through the magnet isocenter and an offset slice passing through the phantom.

3. Analysis

a. Phase-encoding errors. Phase-encoding ghosts will appear as multiple images (possibly smeared into a column) originating at the true object position but displaced along the phase-encoding axis of the image (perpendicular to the frequency encoding direction). The presence of these characteristic ghost images will generally identify the two axes; however, the orientations should be verified by the manufacturer or operator's manual. Regions-of-interest values are taken from both the true image and the brightest ghost image. The magnitude of the error *(E)* is quantified by expressing the ghost ROI value *(G)* as a percent of the true ROI *(T)*:

$$E = \frac{(T-G)}{T} \times 100\%.$$

6. dc-offset errors. dc-offset errors typically appear as a single bright pixel (sometimes as a dark pixel if overflow or processing has occurred) at the center of the image matrix. The existence of this error is assessed visually.

c. Receive quadrature errors. Receive quadrature ghosts will be evaluated using the central slice of the multislice sequence acquire with the phantom at the isocenter. Receive ghosts will appear upside down and reversed from the true signal producing object (object in the upper left-hand corner will appear as a ghost in the lower right-hand corner). Regions-of-interest values are taken from both the true image and the ghost image. The receive quadrature error *(E)* is quantified by expressing the ghost ROI value *(G)* as a percent of the true ROI *(T)*.

$$E = \frac{(T-G)}{T} \times 100\%.$$

d. Transmit quadrature errors. Transmit quadrature ghosts are evaluated using images acquired in multislice mode in which the phantom is placed at a location offset from the isocenter. A transmit ghost appears in the slice located in the opposite offset direction at a distance equal to the distance at which the true object is located from the isocenter (mirror image from the isocenter). The ghost and true object image will be located at the same relative positions in their respective images. For example, a true object

located in the upper left-hand corner at a distance of + 5 cm from the isocenter will produce a transmit quadrature ghost in the upper left-hand corner of the image at - 5 cm. ROI's taken over the true object and the ghost are used to determine the percent error *(E)*.

$$E = \frac{(T - G)}{T} \times 100\%.$$

D. Action criterion

Phase related errors should typically be < 5% of the true signal value. dc-offset errors should not be present in images from a properly functioning system.

Further information on MRI quality assurance methods and phantoms may be found in the scientific literature (7-38).

[a] Task Group No. 1 is part of the AAPM Nuclear Magnetic Resonance Committee, Stephen R. Thomas, Chairman, during development of document (current Chairman Ronald R. Price). This document has been co-sponsored by the American College of Radiology, MR Committee on Imaging Technology and Equipment, Alexander R. Margulis, Chairman.

[1] R. R. Price, J. A. Patton, J. J. Erickson, et al., "Concepts of Quality Assurance and Phantom Design for NMR Systems," Medical Physics Monograph *No.* 14, *NMR in Medicine: The Instrumentation and Clinical Application,* edited by S. R. Thomas and R. L. Dixon, (American Institute of Physics, NY, 1985), p. 414.

[2] M. Bucciolini, L. Ciraolo and R. Renzi, Med. Phys. 13,298-303 (1986).

[3] P. T. Beale, S. R. Amtey, and S. R. Kasturi *NMR Data Handbook for Biomedical Applications* (Pergamon Press, New York, 1984).

[4] William R. Hendee, *Medical Radiation Physics,* "Accumulation and Analysis of Nuclear Data", (Year Book Medical, Chicago, 1979), Chap. 12.

[5] D. I. Hoult, "NMR Imaging Techniques," 40, 132-138 (1984).

[6] D. R. White, R. D. Speller, and P. M. Taylor, "Evaluating Performance Characteristics in Computed Tomography," Br. J. Radiol. 54, 221-231 (1981).

[7] J. M. S. Hutchinson, R. J. Sutherland, and J. R. Mallard "NMR Imaging: Image Recovery Under Magnetic Fields with Large Non-Uniformities," J. Phys. E. Sci. Instrum. 11,217-221 (1978).

[8] Ching-Ming Lai, "Reconstructing NMR Images from Projections under Inhomogeneous Magnetic Field and Non-linear Field Gradients, Phys. Med. Biol. 28, 925-938 (1983).

[9] V. M. Runge, C. T. Johnson, and F. W. Smith, "Phantoms for Magnetic Resonance Imaging," Noninvas. Med. Imag. 1, 49-60 (1984).

[10] I. R. Young, D. J. Bryant, I. A. Payne, "Variations in slice shape and absorption as artifacts in the determination of tissue parameters in NMR Imaging", Magnetic Resonance in Medicine, 2, 355-389 (1985).

[11] M. O'Donnell and W. A. Edelstein, "NMR Imaging in the Presence of Magnetic Field Inhomogeneities and Gradient Field Non-linearities," Med. Phys. 12, 20-26 (1985).

[12] R. A. Lerski, K. Straughan. J. S. Orr, "Calibration of Proton Density Measurements in Nuclear Magnetic Resonance Imaging," Phys. Med. Biol. 271-276 (1986).

[13] W. A. Edelstein, G. H. Glover, C. J. Hardy, R. W. Redington, "The Intrinsic Signal-to-Noise Ratio in NMR Imaging," Magnetic Resonance in Medicine 3, 604-618 (1986).

[14] L. Brateman, L. W. Jennings, R. L. Nunnally, et al., "Evaluations of Magnetic Resonance Imaging Parameters with Simple Phantoms," Med. Phys. 13, 441-448 (1986).

[15] D. W. McRobbie, R. A. Lerski, K. Straughan, "Investigation of Slice Characteristics in Nuclear Magnetic Resonance Imaging. Phys. Med. Biol. 31, 613-626 (1986).

[16] E. M. Bellon, E. M. Haacke, P. E. Coleman, "M. R. Artifacts: A Review," Am. J. of Roent. 147, 1271-1281 (1986).

[17] E. Pusey D. D. Stark, R. B. Lufkin, "Magnetic Resonance Imaging Artifacts: Mechanism and Clinical Significant," Radiographics 6, 891-911 (1986).

[18] R. K. Breger, F. E. W. Wehrli, H. C. Charles, "Reproducibility of Relaxation and Spin Density Parameters in Phantoms and the Human Brain Measured by MR Imaging at 1.5T," Mag. Res. in Med. 3, 649-662 (1986).

[19] I. Mano, H. Goshima, M. Namba, "New Polyvinyl Alcohol Gel Material for MRI Phantoms," Mag. Res. in Med. 3, 921-926 (1986).

[20] J. R. Kowles and J. A. Markisz, "Upholding MR Image Quality can be a Complex but Profitable Pursuit," Diagnostic Imaging 125-130 (1987).

[21] R. M. Henkelman, and M. J. Bronskill, "Artifacts in Magnetic Resonance Imaging," *Reviews of Magnetic Resonance in Medicine: Special Issue,* (Pergamon, New York, 1987), Vol. 2.

[22] J. A. Patton. M. V. Kulkarni, J. K. Craig, "Techniques, Pitfalls and Artifacts in Magnetic Resonance Imaging," Radiographics 7, 505-519 (1987).

[23] J. E. Gray, "Section Thickness and Contiguity Phantom for MR Imaging," Radiology 164, 193-197 (1987).

[24] "Identification and Characterization of Biological Tissue by NMR. Concerted Research Project of the European Economic Community," edited by John C. Gore and Francis W. Smith. Special Editorial Mag. Res. Imag. 6, 171-222 (1988).

[25] "IV. Protocols and Test Objects for the Assessment of MRI Equipment: EEC Concerted Research Project," edited by John C. Gore and Francis W. Smith, Mag. Res. Imag. 6, 195-199 (1988).

[26] R. A. Lerski, D. W. McRobbie, K. Straughan, P. M. Walker, J. D. de Certaines and A. M. Bernard, "V. Multi-Center Trial with Protocols and Prototype Test Objects for the Assessment of MRI Equipment," Mag. Res. Imag. 6, 201-214 (1988).

[27] P. Walker, R. A. Lerski, DeVre-Mathur, J. Binet and F. Yane, "VI. Preparation of Agarose Gels as Reference Substances for NMR Relaxation Time Measurements," Mag. Res. Imag., 6, 215-222 (1988).

[28] J. C. Blechinger, B. C. Madsen and G. R. Frank, "Tissue Mimicking Gelatin-Agar Gels for Use in Magnetic Resonance Imaging Phantoms," Med. Phys., 15.629-636 (1988).

[29] W. A. Edelstein, P. A. Bottomley and L. M. Pfeiffer, A Signal-to-Noise Calibration Procedure for NMR Imaging Systems," Med. Phys. 11, 180-185 (1984).

[30] C. W. Coffey, R. Taylor, C. T. Umstead, "A Slice Geometry Phantom for Cross-Sectional Tomographic Imagers," Med. Phys. 16, 273-278 (1989).

[31] M. Chui, D. Blakesley, S. Mohapata, "Test Method for MR Image Slice Profile," J. Comp. Assist. Tomogr. 9, 1150-1152 (1985).

[32] M. Grey and C. W. Coffey: Method for Evaluating Image Quality in Magnetic Resonance Imaging, Radiol. Technol. 58, 339 (1987).

[33] M. Selikson and T. Fearon, "Averaging Error in NMR Slice Profile Measurements," Magn. Reson. Med. 7, 280 (1988).

[34] B. R. Condon, J. Patterson, D. Wyper, et al., "Image Nonuniformity in Magnetic Resonance Imaging: Its Magnitude and Methods for Correction," Br. J. Radiol., 60, 83-87 (1987).

[35] D. W. McRobbie, "Quality Assurance and Specification Measurements in NMR Imaging," in *Quality Assurance in Medical Imaging,* (The Institute of Physics, Bristol, 1986), pp. 49-66.

[36] M. M. Corell, D. O. Mearshen, P. L. Carson, et al., "Automated Analysis of Multiple Performance Characteristics in Magnetic Resonance Imaging Systems," Med. Phys. 13, 815-823 (1986).

[37] M. E. Masterson et al., "Accuracy and Reproducibility of Image Derived Relaxation Times," Med. Phys. 16, 229-233 (1989).

[38] "MRI: Acceptance Testing and Quality Control," *Proceedings of AAPM Symposium,* Winston-Salem, North Carolina, edited by Robert L. Dixon, (Medical Physics Publishing Corporation, Madison, Wisconsin 1988).